ACS OMEGA

Open Access

http://pubs.acs.org/journal/acsodf

Article

Ratio of the Primers Used in Polymerase Chain Reaction-Stop Analysis Impacts the Resultant Banding Pattern

Lijun Xiang, Xiaojuan Zhang, Sheng Li, Qili Feng, and Kangkang Niu*

Cite This: *ACS Omega* 2023, 8, 37369−37373

Read Online

ACCESS | Metrics & More | Article Recommendations

ABSTRACT: G-quadruplex (G4), as a dynamic nucleic acid secondary structure, widely exists in organism genomes and plays regulatory roles in a variety of cellular functions. Polymerase chain reaction stop assay (PCR-Stop) is a simple, quick, and low-cost widely used method for detection of the binding between G4 and its binding compounds. Different from the common PCR approach, no double-stranded DNA template is needed in the PCR-Stop assay, in which the forward and reverse primers extend against each other in the presence of DNA polymerase to produce a single DNA product. However, unexpected results, such as two or more PCR products, are often generated, and the mechanism is unclear. We found that the ratio of pair primers significantly impacts the generation and components of PCR-Stop products, which is crucial for the interpretation of the experiment results.

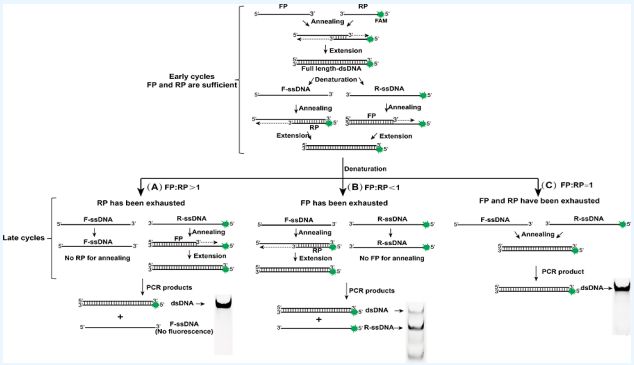

INTRODUCTION

G4 is a dynamic DNA secondary structure, which is more likely formed in the guanine (G)-rich sequences.[1] G4 structure is formed by two or more stacked G-tetrads, which are square coplanar arrays of four guanine bases through eight Hoogsteen hydrogen bonds.[2] In the human genome, more than 376,000 putative quadruplex sequences (PQSs) were predicted.[3,4] Genome-wide prediction revealed that PQSs are enriched in genomic regions associated with gene transcription regulation, DNA duplication, and telomere activities.

G4 ligands, which can bind and stabilize G4 structures in vitro and in vivo, have received extensive attention, and significant progress has been made due to the potential importance of G4 structures in cancer therapeutics. Recently, the first-in-class G4 stabilizer ligand CX-5461 was granted a fast-track designation for the treatment of patients with BRCA1/2, PALB2, or other homologous recombination deficiency (HRD) mutations in their breast or ovarian cancer that acts in tandem with HR pathway deficiency.[5] QN-302, a G4-selective transcription inhibitor, has been developed as a potential treatment for pancreatic ductal adenocarcinoma.[6] The database G4LDB 2.2 collected 3099 G4 binding ligands and 4751 corresponding complexes and their activity records.[7] Increasing G4 ligands are actively advanced toward the clinical trials stage. Verification of the binding specificity between G4 and its ligand appears to be particularly important for drug development.

The PCR-Stop assay has been widely used to identify G4 ligands.[8−10] In the assay, the forward primer (FP) containing the PQS is amplified with a complementary reverse primer (RP), which is overlapped with the FP in the last G-tract region, under DNA polymerase catalyzation to produce a single double-stranded PCR product (Figure 1A). In the presence of a G4 ligand, the PQS containing FP is stabilized to form a G4 structure, impairing RF annealing and PCR amplification. The binding potency of G4 ligands 12459, telomestatin, BRACO19, and TMPyP4 to several different G4s (G4TERT1, G4TERT2, and VNTR6−1) was determined by using this PCR-Stop assay.[11] In leukemia cells, Pu22 oligomer G4 was induced by G4 ligand SYUIQ-5, as detected by PCR-Stop, leading to delayed apoptosis of leukemia cells.[12] In general, PCR-Stop has become an effective and efficient method to detect the interaction of the G4 structure and G4 ligand and is used to screen G4 ligands. However, the PCR-Stop assay may also generate some confused and puzzled results; for example, more than one PCR product band was generated[13−16] when the FP and RP were annealed. It is generally believed that the appearance of multiple bands is caused by nonspecific amplification due to complementary characteristics of the FP and RP or low annealing temper-

Received: July 19, 2023
Accepted: September 14, 2023
Published: September 25, 2023

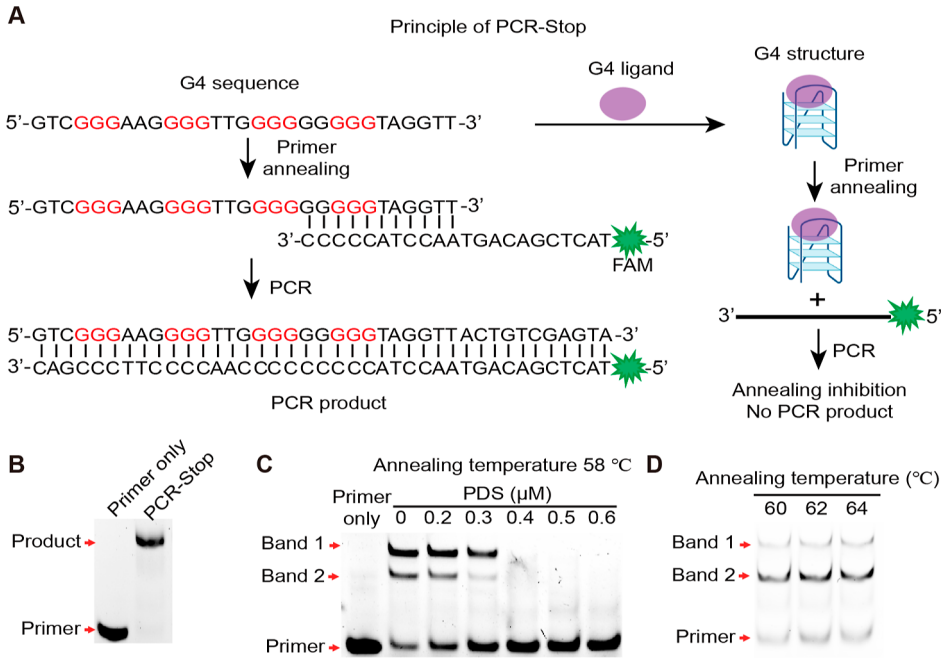

Figure 1. Formation and stabilization of the BmACBP G4 structure induced by PDS were analyzed by PCRStop. (A) Principle of PCR-Stop analysis. (B) PCR-Stop products in normal condition. (C) PCR-Stop analysis with different concentrations of PDS. (D) Effects of different annealing temperatures on PCR products.

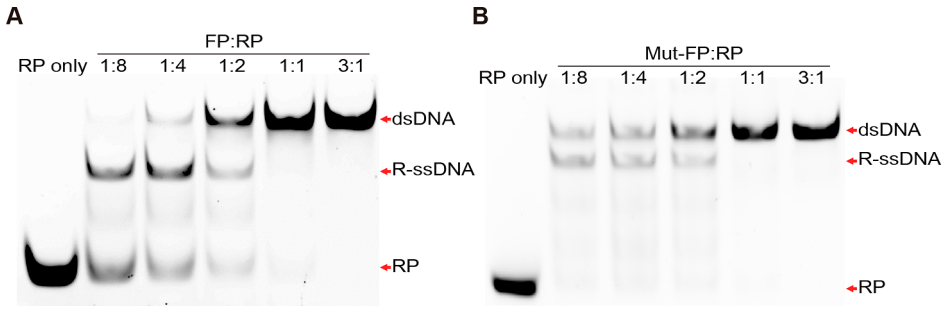

Figure 2. Effects of different ratios of the FP and RP on PCR products. (A) Wild-type FP containing a G4 sequence was used. (B) Mutant FP without a G4 sequence was used.

atures. In this paper, we found that the different ratios of FP and RP are the major factor in the polymorphism of PCR products in this assay.

RESULTS

Two Bands Produced in PCR-Stop Analysis. In our previous study, we identified a G4 structure in the promoter of the ACBP gene in *Bombyx mori*.[17] To further analyze whether pyridostatin (PDS), a well-known G4 inducer and stabilizer, could bind and stabilize this G4 structure, we performed PCR-Stop analysis with the ACBP G4 containing FP and the partially complementary and FAM-labeled RP (Figure 1A). In normal conditions, a single PCR product should be generated, as expected (Figure 1B). However, in some cases, two PCR products were found (Figure 1C), with the larger product being the full-length PCR product and the smaller one being the unknown product. This unexpected result was also detected in many other PCR-Stop experiments,[13−16] indicating that this phenomenon was not accidental.

When PDS was added to the reaction system at 58 °C, the generation of the two PCR products was suppressed with the increase in the PDS concentration (Figure 1C). When the concentration of PDS was at 0.4 μM or higher, no PCR product was detected, indicating that PDS induced the formation of the G4 structure in the FP so that PCR was inhibited.

For the two PCR products, we first speculate whether they might be due to the shifted annealing of the two primers. To test this, we conducted PCR with a gradually increased annealing temperature, given that an elevated annealing temperature could reduce nonspecific amplification. The result showed that when the annealing temperatures were increased from 58 to 64 °C, the two PCR products were still detected (Figure 1D), suggesting that the appearance of the two PCR products was not due to shifted annealing of the primers.

Effects of Different Ratios of FP and RP on PCR Products. The PCR-Stop analysis is different from common PCR, and no double-stranded DNA template is needed. The forward and reverse primers are used as mutual templates for each other in the annealing and extension reactions. Thus, the ratios of FP and RP used in the initial reaction are critical for the reaction products (abstract graphics). To further verify these results and analysis, we performed PCR at 58 °C with different ratios of the FP and RP. The results showed that

https://doi.org/10.1021/acsomega.3c05220
ACS Omega 2023, 8, 37369−37373

when FP/RP < 1 (1:8, 1:4, and 1:2), two PCR product bands were observed, while when FP/RP ≥ 1(1:1 and 3:1), a unique PCR product band was obtained (Figure 2A). Additionally, to exclude possible effects of the G4 structure, we conducted PCR with the mutant FP that could not form the G4 structure. The result was consistent with that when the wild-type FP was used (Figure 2B). These results clearly demonstrated that different ratios of FR and RP resulted in different PCR product patterns.

Further Confirmation of ssDNA. To further confirm the above results, fluorescence-labeled R-ssDNA was synthesized and run on a gel along with the PRC-Stop products. The result of electrophoresis showed that the size of the R-ssDNA band obtained in the PCR-Stop was exactly the same as that of the synthesized fluorescence-linked R-ssDNA (Figure 3). Furthermore, we treated the PCR-Stop products with S1 nuclease, which degrades ssDNA with much higher activity than dsDNA.[18] The results show that the R-ssDNA, as well as the single-stranded RP, disappeared after the S1 nuclease treatment, confirming that the smaller band was the R-ssDNA molecules generated during PCR-Stop amplification.

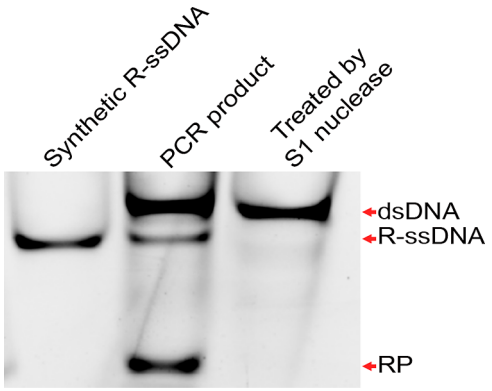

Figure 3. Size comparison of the synthesized fluorescence-labeled R-ssDNA and the R-ssDNA obtained in the PCR-Stop assay and digestion by S1 nuclease.

DISCUSSION

Since the discovery of the G-tetrad structure in 1962, the structures and functions of G4 in organisms have become more and more attractive.[1,18] A variety of diseases, such as cancer, nervous system disease, and chondropathy, have been found to be related to G4 structures[1,19,20] and G4 structures are potential targets for disease treatment. Many small chemical molecules that specifically target and bind to G4, named G4 ligands, have been selected to disturb G4. For instance, the treatment of neurological diseases caused by the C9ORF72 mutation.[21,22] In 2022, the Food and Drug Administration (FDA) of the United States granted fast-track designation to CX-5461 for the treatment of certain patients with breast or ovarian cancer.[5] In 2023, the FDA granted orphan drug designation to QN-302 for the management of pancreatic cancer.[6] With the application of G4 as a drug target, screening and identification of G4 ligands have become increasingly critical.

So far, the main detection methods for studying the interaction between G4 structures and G4 ligands can be divided into biophysical and molecular biology methods. Biophysics approaches include structure-based methods (such as circular dichroism, nuclear magnetic resonance, and X-ray crystallography), affinity and apparent affinity-based methods (such as surface plasmon resonance and isothermal titration calorimetry), and high-throughput methods (such as fluorescence resonance energy transfer-melting, fluorescence intercalator displacement, affinity chromatography, and microarrays).[23] Molecular biology methods include the electrophoretic mobility shift assay, the PCR-Stop assay, and the polymerase stop assay.[24] All of these methods contribute to the study of the interaction between G4 and its ligands, but each individual method is not comprehensive and has its own advantages and disadvantages. PCR-Stop is a classical research method that is effective and efficient. The results can be obtained with an ordinary gel imaging system. In addition, the mutant primers can be designed to exclude the influence of the tested drug on the polymerase and avoid the occurrence of false positives.

Although PCR-Stop has been widely used for analysis of interaction between G4 structures and G4 ligands, most of the results displayed either an incomplete gel image[11,25] or contained multiple PCR product bands.[13−16] In this study, we found that the ratio of the forward primer and reverse primer was responsible for the occurrence of multiple product bands. When the amount of the forward primer was more than that of the reverse primer, a mixture of full-length double-stranded DNA products and the single-stranded DNA amplification product of the forward primer was generated. Oppositely, when the amount of the reverse primer was greater than that of the forward primer, a mixture of full-length double-stranded DNA products and a single-stranded DNA amplification product was produced. When the amounts of the forward primer and reverse primer are completely the same, full-length double-stranded DNA molecules are the unique product. In these cases, nonspecific binding or annealing of the primers to each other was not a main contributor to the multiple PCR products when no G4 ligand was present.

PCR-Stop DNA products can be detected either by nucleic acid dyes or by fluorescent labeling.[16,17,25−27] Since a nucleic acid dye can usually stain both single- and double-stranded DNA, it can display more complex banding patterns than fluorescent labeling, in which the reverse primers are usually labeled.[28,29] Our experimental results demonstrated that using fluorescent labeling in PCR-Stop research to study the binding of drugs with G4 is more sensitive and convenient compared with the traditional DNA-binding dye. When visualizing PCR products with DNA-binding dye, the FP/RP ratio should strictly be 1. However, deviations in the FP/RP ratio can occur due to operational errors or issues with primer quality, leading to the appearance of extra bands caused by incomplete synthesis products.[13−16] The fluorescent labeling can make the range of effective primer FP/RP ratios wider and allow them to exceed 1 in order to avoid the generation of multiple bands. In particular, when calculating the binding constant with PCR-Stop results, misjudgment of double-stranded product bands may lead to objectively erroneous results. The brightest band was regarded as a double-stranded product, but our results indicate that the single-stranded product exhibits higher brightness than the double-stranded product when FP/RP < 1.

In conclusion, in the PCR-Stop assay for detection of the binding of G4 structure and G4 ligand, multiple PCR products mostly result from unequal dose use of forward and reverse primers in the reaction system, which should be avoided to obtain clear and interpretable results.

https://doi.org/10.1021/acsomega.3c05220
ACS Omega 2023, 8, 37369−37373

Table 1. Sequences of the Synthesized Oligonucleotides

name	sequence
FAM-labeled RP	5′ FAM -TACTCGACAGTAACCTACCCCC-3′
unlabeled wild type FP	5′-GTCGGGAAGGGGTTGGGGGGGGGTAGGTT-3′
unlabeled mutant FP	5′-GTCGTGAAGGTGTTGATGGGGGGTAGGTT-3′
FAM-labeled reverse−ssDNA (R-ssDNA)	5′FAM-TACTCGACAGTAACCTACCCCCCCCCAACCCCTTCCCGAC-3′

METHODS

Oligonucleotide Synthesis and Labeling. The target sequence of this study was the G4 sequence of the BmACBP.[17] Oligonucleotides labeled with 5′FAM (6-carboxyfluorescein) were synthesized by Tsingke Biotechnology Co., Ltd. (Nanjing, China). The sequences of the synthesized oligonucleotides are listed in Table 1. The synthesized oligonucleotides were dissolved in ddH_2O at a concentration of 10 μM.

G4 Formation and Pyridostatin (PDS) Treatment. The sense strand of the wild-type or mutated BmACBP G4 DNA sequences was used as FP. Antisense strands of the wild-type or mutated BmACBP G4 DNA sequences were used as RP. The forward primers dissolved in 50 mM Tris-HCl (pH 7.4) with 100 mM KCl were heated at 95 °C for 10 min and then slowly cooled to room temperature to allow G4 structure formation. For PDS treatment, the annealed forward primer was incubated with different amounts of PDS (MCE, NJ, USA) for 30 min at room temperature before the PCR assay. Dimethyl sulfoxide (DMSO) treatment was used as control.

PCR-Stop Assay. All reactions were performed in a final volume of 20 μL of the reaction system. The composition has been listed in Table 2. The PCR reaction was conducted according to the procedure listed in Table 3. The PCR products were detected by electrophoresis on a 15% denaturing polyacrylamide gel.

Table 2. Composition of the Reaction System in the PCR−stop Assay

component	dosage
PCR buffer	1× (10 mM Tris-HCl, 50 mM KCl, 1.5 mM $MgCl_2$)
dNTPs	0.25 mM
Taq DNA polymerase	2 units
RP	2.5 pmol
FP	FP as adjuncts in different proportions with RP
ddH_2O	add to 20 μL

Table 3. PCR Procedure Used in the PCR-Stop Assay

temperature (°C)	time (min)/cycle	
95	3	
95	0.5	30 cycles
58	0.5	
72	0.5	

S1 nuclease Digestion. PCR-Stop products were digested with S1 nuclease (Promega Corp., Madison, W; 2 units) in 1× S1 reaction buffer (0.5 M sodium acetate pH 4.5, 2.8 M NaCl, 45 mM $ZnSO_4$) at 37 °C for 5 min. The digestion products were detected by electrophoresis on a 15% denaturing polyacrylamide gel.

AUTHOR INFORMATION

Corresponding Author

Kangkang Niu − *Guangdong Provincial Key Laboratory of Insect Developmental Biology and Applied Technology, Guangzhou Key Laboratory of Insect Development Regulation and Application Research, Institute of Insect Science and Technology, School of Life Sciences, South China Normal University, Guangzhou 510631, China;* orcid.org/0000-0002-0050-5741; Email: kkniu@m.scnu.edu.cn

Authors

Lijun Xiang − *Guangdong Provincial Key Laboratory of Insect Developmental Biology and Applied Technology, Guangzhou Key Laboratory of Insect Development Regulation and Application Research, Institute of Insect Science and Technology, School of Life Sciences, South China Normal University, Guangzhou 510631, China*

Xiaojuan Zhang − *Guangdong Provincial Key Laboratory of Insect Developmental Biology and Applied Technology, Guangzhou Key Laboratory of Insect Development Regulation and Application Research, Institute of Insect Science and Technology, School of Life Sciences, South China Normal University, Guangzhou 510631, China*

Sheng Li − *Guangdong Provincial Key Laboratory of Insect Developmental Biology and Applied Technology, Guangzhou Key Laboratory of Insect Development Regulation and Application Research, Institute of Insect Science and Technology, School of Life Sciences, South China Normal University, Guangzhou 510631, China; Guangmeiyuan R&D Center, Guangdong Provincial Key Laboratory of Insect Developmental Biology and Applied Technology, South China Normal University, Meizhou 514779, China*

Qili Feng − *Guangdong Provincial Key Laboratory of Insect Developmental Biology and Applied Technology, Guangzhou Key Laboratory of Insect Development Regulation and Application Research, Institute of Insect Science and Technology, School of Life Sciences, South China Normal University, Guangzhou 510631, China*

Complete contact information is available at: https://pubs.acs.org/10.1021/acsomega.3c05220

Author Contributions

K.N. supervised the project. L.X. performed all of the experiments. K.N. and X.Z. analyzed the data and created all of the figures. K.N., X.Z., S.L., and Q.F. wrote and edited the manuscript.

Notes

The authors declare no competing financial interest.

ACKNOWLEDGMENTS

This work was supported by the National Natural Science Foundation of China (31930102, 32250710148, 32000337, and 32102610).

https://doi.org/10.1021/acsomega.3c05220
ACS Omega 2023, 8, 37369−37373

REFERENCES

(1) Varshney, D.; Spiegel, J.; Zyner, K.; Tannahill, D.; Balasubramanian, S. The regulation and functions of DNA and RNA G-quadruplexes. *Nat. Rev. Mol. Cell Biol.* **2020**, *21*, 459−474.

(2) Sen, D.; Gilbert, W. A sodium-potassium switch in the formation of four-stranded G4-DNA. *Nature* **1990**, *344*, 410−414.

(3) Huppert, J. L.; Balasubramanian, S. Prevalence of quadruplexes in the human genome. *Nucleic Acids Res.* **2005**, *33*, 2908−2916.

(4) Todd, A. K.; Johnston, M.; Neidle, S. Highly prevalent putative quadruplex sequence motifs in human DNA. *Nucleic Acids Res.* **2005**, *33*, 2901−2907.

(5) Hilton, J.; Gelmon, K.; Bedard, P. L.; Tu, D.; Xu, H.; Tinker, A. V.; Goodwin, R.; Laurie, S. A.; Jonker, D.; Hansen, A. R.; Veitch, Z. W.; Renouf, D. J.; Hagerman, L.; Lui, H.; Chen, B.; Kellar, D.; Li, I.; Lee, S. E.; Kono, T.; Cheng, B. Y. C.; Yap, D.; Lai, D.; Beatty, S.; Soong, J.; Pritchard, K. I.; Soria-Bretones, I.; Chen, E.; Feilotter, H.; Rushton, M.; Seymour, L.; Aparicio, S.; Cescon, D. W. Results of the phase I CCTG IND.231 trial of CX-5461 in patients with advanced solid tumors enriched for DNA-repair deficiencies. *Nat. Commun.* **2022**, *13*, 3607.

(6) Ahmed, A. A.; Greenhalf, W.; Palmer, D. H.; Williams, N.; Worthington, J.; Arshad, T.; Haider, S.; Alexandrou, E.; Guneri, D.; Waller, Z. A. E.; Neidle, S. The Potent G-Quadruplex-Binding Compound QN-302 Downregulates S100P Gene Expression in Cells and in an In Vivo Model of Pancreatic Cancer. *Molecules* **2023**, *28*, 2452.

(7) Wang, Y. H.; Yang, Q. F.; Lin, X.; Chen, D.; Wang, Z. Y.; Chen, B.; Han, H. Y.; Chen, H. D.; Cai, K. C.; Li, Q.; Yang, S.; Tang, Y. L.; Li, F. G4LDB 2.2: a database for discovering and studying G-quadruplex and i-Motif ligands. *Nucleic Acids Res.* **2022**, *50*, D150−D160.

(8) Yu, Q.; Liu, Y.; Zhang, J.; Yang, F.; Sun, D.; Liu, D.; Zhou, Y.; Liu, J. Ruthenium(II) polypyridyl complexes as G-quadruplex inducing and stabilizing ligands in telomeric DNA. *Metallomics* **2013**, *5*, 222−231.

(9) Verma, S. P.; Das, P. Novel splicing in IGFN1 intron 15 and role of stable G-quadruplex in the regulation of splicing in renal cell carcinoma. *PLoS One* **2018**, *13*, No. e0205660.

(10) Lin, J.; Hou, J. Q.; Xiang, H. D.; Yan, Y. Y.; Gu, Y. C.; Tan, J. H.; Li, D.; Gu, L. Q.; Ou, T. M.; Huang, Z. S. Stabilization of G-quadruplex DNA by C-5-methyl-cytosine in bcl-2 promoter: implications for epigenetic regulation. *Biochem. Biophys. Res. Commun.* **2013**, *433*, 368−373.

(11) Gomez, D.; Lemarteleur, T.; Lacroix, L.; Mailliet, P.; Mergny, J. L.; Riou, J. F. Telomerase downregulation induced by the G-quadruplex ligand 12459 in A549 cells is mediated by hTERT RNA alternative splicing. *Nucleic Acids Res.* **2004**, *32*, 371−379.

(12) Liu, J. N.; Deng, R.; Guo, J. F.; Zhou, J. M.; Feng, G. K.; Huang, Z. S.; Gu, L. Q.; Zeng, Y. X.; Zhu, X. F. Inhibition of myc promoter and telomerase activity and induction of delayed apoptosis by SYUIQ-5, a novel G-quadruplex interactive agent in leukemia cells. *Leukemia* **2007**, *21*, 1300−1302.

(13) Yildiz, U.; Kandemir, I.; Comert, F.; Akkoc, S.; Coban, B. Synthesis of naphthalimide derivatives with potential anticancer activity, their comparative ds- and G-quadruplex-DNA binding studies and related biological activities. *Mol. Biol. Rep.* **2020**, *47*, 1563−1572.

(14) Ma, H.; Zhang, M.; Zhang, D.; Huang, R.; Zhao, Y.; Yang, H.; Liu, Y.; Weng, X.; Zhou, Y.; Deng, M.; Xu, L.; Zhou, X. Pyridyl-substituted corrole isomers: synthesis and their regulation to G-quadruplex structures. *Chem.−Asian J.* **2010**, *5*, 114−122.

(15) Ya-Xuan, M.; Shuang, W.; Shuang-Mei, Y.; Yue, C.; Ming-He, W.; Ze-bao, Z.; Xiao-Long, Z. INDUCTION OF C-MYC G-QUADRUPLEX DNA AND CYTOTOXICITY OF A CALIX[4]-ARENE-CONTAINING BINUCLEAR RUTHENIUM(II) COMPLEX. *J. Chil. Chem. Soc.* **2019**, *64*, 4639.

(16) Ramos, C. I. V.; Almodovar, V. A. S.; Candeias, N. R.; Santos, T.; Cruz, C.; Neves, M.; Tome, A. C. Diketopyrrolo[3,4-c]pyrrole derivative as a promising ligand for the stabilization of G-quadruplex DNA structures. *Bioorg. Chem.* **2022**, *122*, 105703.

(17) Xiang, L.; Niu, K.; Peng, Y.; Zhang, X.; Li, X.; Ye, R.; Yu, G.; Ye, G.; Xiang, H.; Song, Q.; Feng, Q. DNA G-quadruplex structure participates in regulation of lipid metabolism through acyl-CoA binding protein. *Nucleic Acids Res.* **2022**, *50*, 6953−6967.

(18) Vogt, V. M. Purification and further properties of single-strand-specific nuclease from Aspergillus oryzae. *Eur. J. Biochem.* **1973**, *33*, 192−200.

(19) Wang, E.; Thombre, R.; Shah, Y.; Latanich, R.; Wang, J. G-Quadruplexes as pathogenic drivers in neurodegenerative disorders. *Nucleic Acids Res.* **2021**, *49*, 4816−4830.

(20) Tian, Y.; Wang, W.; Lautrup, S.; Zhao, H.; Li, X.; Law, P. W. N.; Dinh, N. D.; Fang, E. F.; Cheung, H. H.; Chan, W. Y. WRN promotes bone development and growth by unwinding SHOX-G-quadruplexes via its helicase activity in Werner Syndrome. *Nat. Commun.* **2022**, *13*, 5456.

(21) Haeusler, A. R.; Donnelly, C. J.; Periz, G.; Simko, E. A.; Shaw, P. G.; Kim, M. S.; Maragakis, N. J.; Troncoso, J. C.; Pandey, A.; Sattler, R.; Rothstein, J. D.; Wang, J. C9orf72 nucleotide repeat structures initiate molecular cascades of disease. *Nature* **2014**, *507*, 195−200.

(22) Zhang, K.; Donnelly, C. J.; Haeusler, A. R.; Grima, J. C.; Machamer, J. B.; Steinwald, P.; Daley, E. L.; Miller, S. J.; Cunningham, K. M.; Vidensky, S.; Gupta, S.; Thomas, M. A.; Hong, I.; Chiu, S. L.; Huganir, R. L.; Ostrow, L. W.; Matunis, M. J.; Wang, J.; Sattler, R.; Lloyd, T. E.; Rothstein, J. D. The C9orf72 repeat expansion disrupts nucleocytoplasmic transport. *Nature* **2015**, *525*, 56−61.

(23) Santos, T.; Salgado, G. F.; Cabrita, E. J.; Cruz, C. G-Quadruplexes and Their Ligands: Biophysical Methods to Unravel G-Quadruplex/Ligand Interactions. *Pharmaceuticals* **2021**, *14*, 769.

(24) Mishra, S. K.; Jain, N.; Shankar, U.; Tawani, A.; Sharma, T. K.; Kumar, A. Characterization of highly conserved G-quadruplex motifs as potential drug targets in Streptococcus pneumoniae. *Sci. Rep.* **2019**, *9*, 1791.

(25) Mishra, S. K.; Shankar, U.; Jain, N.; Sikri, K.; Tyagi, J. S.; Sharma, T. K.; Mergny, J. L.; Kumar, A. Characterization of G-Quadruplex Motifs in espB, espK, and cyp51 Genes of Mycobacterium tuberculosis as Potential Drug Targets. *Mol. Ther. Nucleic Acids* **2019**, *16*, 698−706.

(26) Pandya, N.; Rani, R.; Kumar, V.; Kumar, A. Discovery of a potent Guanidine derivative that selectively binds and stabilizes the human BCL-2 G-quadruplex DNA and downregulates the transcription. *Gene* **2023**, *851*, 146975.

(27) Niu, K.; Xiang, L.; Jin, Y.; Peng, Y.; Wu, F.; Tang, W.; Zhang, X.; Deng, H.; Xiang, H.; Li, S.; Wang, J.; Song, Q.; Feng, Q. Identification of LARK as a novel and conserved G-quadruplex binding protein in invertebrates and vertebrates. *Nucleic Acids Res.* **2019**, *47*, 7306−7320.

(28) Vardevanyan, P. O.; Antonyan, A. P.; Parsadanyan, M. A.; Davtyan, H. G.; Karapetyan, A. T. The binding of ethidium bromide with DNA: interaction with single- and double-stranded structures. *Exp. Mol. Med.* **2003**, *35*, 527−533.

(29) Sapia, R. J.; Campbell, C.; Reed, A. J.; Tsvetkov, V. B.; Gerasimova, Y. V. Interaction of GelRed with single-stranded DNA oligonucleotides: Preferential binding to thymine-rich sequences. *Dyes Pigm.* **2021**, *188*, 109209.

https://doi.org/10.1021/acsomega.3c05220
ACS Omega 2023, 8, 37369−37373